astronomy

MDPI

Article

Isoscalar Giant Monopole Resonance in Spherical Nuclei as a Nuclear Matter Incompressibility Indicator

Mitko K. Gaidarov *, Martin V. Ivanov, Yordan I. Katsarov and Anton N. Antonov

Institute for Nuclear Research and Nuclear Energy, Bulgarian Academy of Sciences, 1784 Sofia, Bulgaria
* Correspondence: gaidarov@inrne.bas.bg

Abstract: The incompressibility of both nuclear matter and finite nuclei is estimated by the monopole compression modes in nuclei in the framework of a nonrelativistic Hartree–Fock–Bogoliyubov method and the coherent density fluctuation model. The monopole states originate from vibrations of the nuclear density. The calculations in the model for the incompressibility in finite nuclei are based on the Brueckner energy–density functional for nuclear matter. Results for the energies of the breathing vibrational states and finite nuclei incompressibilities are obtained for various nuclei and their values are compared with recent experimental data. The evolution of the isoscalar giant monopole resonance (ISGMR) along Ni, Sn, and Pb isotopic chains is discussed. This approach can be applied to analyses of neutron stars properties, such as incompressibility, symmetry energy, slope parameter, and other astrophysical quantities, as well as for modelling dynamical behaviors within stellar environments.

Keywords: nuclear matter; finite nuclei; incompressibility; equation of state; symmetry energy; energy-density functional; nuclear monopole excitations

1. Introduction

In recent years, experimental and theoretical studies of giant resonances have become a rich source of information on the collective response of the nucleus to its density fluctuations [1,2]. In particular, the isoscalar giant monopole resonance (ISGMR) plays an important role in constraining the nuclear equation of state (EOS) [2–7]. An important issue is that the energy of this resonance is closely related to the nuclear incompressibility. The latter can be connected to the incompressibility of the infinite nuclear matter, which represents an important ingredient of the nuclear matter EOS. It is well known that the EOS plays a crucial role in the description of astrophysical quantities, such as radii and masses of neutron stars, the collapse of the heavy stars in super novae explosions, as well as in modeling of heavy-ion collision. The 20% uncertainty of the currently accepted value of the incompressibility of nuclear matter is largely driven by the poor determination of the EOS isospin asymmetry term. Therefore, to make this term more precise, recent experimental measurements of isoscalar monopole modes are being extended in isotopic chains from the nuclei on the valley of stability towards exotic nuclei with larger proton–neutron asymmetry.

The isoscalar resonances are excited through low-momentum transfer reactions in inverse kinematics, that require special detection devices. At present, promising results have been obtained using active targets. Different measurements have been conducted on Ni isotopes far from stability, namely ^{56}Ni [8,9] and ^{68}Ni [10,11]. In particular, the ^{68}Ni experiment is the first measurement of the isoscalar monopole response in a short-lived neutron-rich nucleus using inelastic alpha-particle scattering. The peak of the ISGMR was found to be fragmented, indicating a possibility for a soft monopole resonance.

The discussion on how to extract the incompressibility of nuclear matter ΔK^{NM} from the ISGMR dates back to the years 1980s [12] (see also more recent review [13]).

check for updates

Citation: Gaidarov, M.K.; Ivanov, M.V.; Katsarov, Y.I.; Antonov, A.N. Isoscalar Giant Monopole Resonance in Spherical Nuclei as a Nuclear Matter Incompressibility Indicator. *Astronomy* **2023**, 2, 1–13. https://doi.org/10.3390/astronomy2010001

Received: 27 July 2022
Revised: 27 September 2022
Accepted: 4 January 2023
Published: 12 January 2023

The measurement of the centroid energy of the ISGMR [14–20] provides a very sensitive method to determine the value of ΔK^{NM}. Theoretical investigations in various models [21–27] with grouped values of the nuclear matter incompressibility ΔK^{NM} predict different ISGMR energies. In comparison with the experimental data, one could give the constraint on the nuclear matter incompressibility.

In the present work, the incompressibility and the centroid energy of ISGMR are investigated for three isotopic chains on the basis of the Brueckner energy-density functional for nuclear matter [28,29] and using the coherent density fluctuation model (CDFM) (e.g., Refs. [30–37]). This method is a natural extension of the Fermi gas model based on the delta-function limit of the generator coordinate method [36–38] and includes long-range correlations of collective type. During the years the CDFM has been successfully applied to calculations of nuclear structure and nuclear reactions characteristics. Among them we would like to note the calculated energies, density distributions and rms radii of the ground state in ^{4}He, ^{16}O, and ^{40}Ca nuclei [39]. Here, we mention particularly the calculations within the CDFM of the energies of breathing monopole states in ^{16}O, ^{40}Ca, ^{90}Zr, ^{116}Sn, and ^{208}Pb performed in Ref. [40] and presented also in Chapter 8 of Ref. [37]. In the latter are also given references for experimental data and other theoretical results available until the early 1990s. Concerning the reaction properties, the CDFM has been employed in Refs. [41,42] to calculate the scaling function in nuclei using the relativistic Fermi gas scaling function, which has been applied to lepton scattering processes [41–47]. In addition, information about the role of the nucleon momentum and density distributions for the explanation of superscaling in lepton–nucleus scattering has been obtained [42,43], also in studies of cross sections for several reactions: inclusive electron scattering in the quasielastic and Δ regions [44,45] and neutrino (antineutrino) scattering both for charge-changing [45,47] and for neutral-current [46,47] processes. Furthermore, the CDFM was applied to study the scaling function and its connection with the spectral function and the nucleon momentum distribution [48].

The efficiency of CDFM to be applied as a "bridge" for a transition from the properties of nuclear matter to the properties of finite nuclei studying the nuclear symmetry energy (NSE), the neutron pressure, and the asymmetric compressibility in finite nuclei was demonstrated in our previous works [49–56]. Although there is enough collected information for the mentioned EOS quantities, the volume and surface symmetry energies have been poorly investigated till now. In Ref. [57] we proposed a new alternative approach to calculate the ratio of the surface to volume components of the NSE in the framework of the CDFM. We have demonstrated that the new scheme provides more realistic values, in a better agreement with the empirical data, and exhibits correct conceptual advantages.

In this work, we perform calculations and give results for the excitation energies of ISGMR for Ni, Sn, and Pb isotopes. Our main task is to validate the CDFM for studies of collective vibrational modes by using as a main theoretical ground the self-consistent Hartree–Fock (HF)+BCS method with Skyrme interactions. The mentioned above model gives a link between nuclear matter and finite nuclei in studying of their properties, such as binding energies and rms radii of light, medium, and heavy nuclei. As an example, for nuclear matter we adopt the energy-density functional (EDF) of Brueckner et al. [28,29]. Obviously, more realistic functionals should be employed in the future studies which would lead to values of the excitation energies of ISGMR that are in better agreement with the experimental ones. More details on this point are given in the last section of the work, where specific future improvements are pointed out. We present and discuss the values of the centroid energies in Sn isotopic chain (A = 112–124) studying its isotopic sensitivity. The main reason to select these chains of spherical nuclei is partly supported by their recent intensive ISGMR measurements so that we focus too on the comparison with the available experimental data for Ni [58], Sn [59], and Pb [60,61] isotopes.

In the next Section 2 we give definitions of the excitation energy of ISGMR and EOS parameters of nuclear matter that characterize its density dependence around normal nuclear matter density, as well as a brief description of the CDFM formalism that provides a way to calculate the finite nuclei quantities. The numerical results are presented and discussed in Section 3. The main conclusions of the study are summarized in Section 4.

2. Theoretical Formalism

2.1. Excitation Energy of the ISGMR

The centroid energy of ISGMR, E_{ISGMR} is generally related to a finite nucleus incompressibility $\Delta K(N,Z)$ for a nucleus with Z protons and N neutrons ($A = Z + N$ is the mass number). Among the various definitions of E_{ISGMR} we will mention the one from, e.g., Ref. [21]):

$$E_{ISGMR} = \frac{\hbar}{r_0 A^{1/3}} \sqrt{\frac{\Delta K(N,Z)}{m}}, \tag{1}$$

where r_0 is deduced from the equilibrium density and m is the nucleon mass. The excitation energy of the ISGMR is also expressed in the scaling model [62] as (in Refs. [15,16], for instance)

$$E_{ISGMR} = \hbar \sqrt{\frac{\Delta K(N,Z)}{m < r^2 >}}, \tag{2}$$

where $< r^2 >$ denotes the mean square mass radius of the nucleus in the ground state. Depending on the adopted model, the value of E_{ISGMR} is associated with different moment ratios of the ISGMR strength distribution. Its extraction is the main focus of the experiments, which aim to constrain the incompressibility of the infinite nuclear matter and, as a consequence, the EOS [13]. Particularly, it should be noticed that definition (2) is usable under the assumption that the strength distribution of a given multipolarity of the resonance is contained within a single collective peak [18].

2.2. The Key EOS Parameters in Nuclear Matter

The symmetry energy $S(\rho)$ is defined by the energy per particle for nuclear matter (NM) $E(\rho,\delta)$ in terms of the isospin asymmetry $\delta = (\rho_n - \rho_p)/\rho$

$$S(\rho) = \frac{1}{2} \frac{\partial^2 E(\rho,\delta)}{\partial \delta^2}\bigg|_{\delta=0}, \tag{3}$$

where

$$E(\rho,\delta) = E(\rho,0) + S(\rho)\delta^2 + O(\delta^4) + \cdots \tag{4}$$

and $\rho = \rho_n + \rho_p$ is the baryon density with ρ_n and ρ_p denoting the neutron and proton densities, respectively (see, e.g., [57,63,64]).

The incompressibility (the curvature) of the symmetry energy ΔK^{NM} is given by

$$\Delta K^{NM} = 9\rho_0^2 \frac{\partial^2 S}{\partial \rho^2}\bigg|_{\rho=\rho_0}, \tag{5}$$

where ρ_0 is the density at equilibrium.

2.3. The EOS Parameters of Finite Nuclei in the Coherent Density Fluctuation Model

The CDFM was suggested and developed in Refs. [30–37] (see also our recent papers [50,54,57]). In it the one-body density matrix (OBDM) of the nucleus $\rho(\mathbf{r},\mathbf{r}')$

$$\rho(\mathbf{r},\mathbf{r}') = \int_0^\infty dx |F(x)|^2 \rho_x(\mathbf{r},\mathbf{r}') \tag{6}$$

is expressed by OBDM's of spherical "pieces" of nuclear matter ("fluctons") with radius x of all A nucleons uniformly distributed in it:

$$\rho_x(\mathbf{r},\mathbf{r}') = 3\rho_0(x) \frac{j_1(k_F(x)|\mathbf{r}-\mathbf{r}'|)}{(k_F(x)|\mathbf{r}-\mathbf{r}'|)} \Theta\left(x - \frac{|\mathbf{r}+\mathbf{r}'|}{2}\right). \tag{7}$$

In Equation (7) j_1 is the first-order spherical Bessel function and

$$k_F(x) = \left(\frac{3\pi^2}{2}\rho_0(x)\right)^{1/3} \equiv \frac{\alpha}{x} \tag{8}$$

is the Fermi momentum with

$$\alpha \equiv \left(\frac{9\pi A}{8}\right)^{1/3} \simeq 1.52A^{1/3}. \tag{9}$$

It can be seen from Equation (6) that the density distribution in the CDFM is:

$$\rho(\mathbf{r}) = \int_0^\infty dx|F(x)|^2\rho_0(x)\Theta(x - |\mathbf{r}|) \tag{10}$$

with

$$\rho_0(x) = \frac{3A}{4\pi x^3}. \tag{11}$$

It follows from Equation (10) that the weight function $|F(x)|^2$ of CDFM can be obtained in the case of monotonically decreasing local densities (i.e., for $d\rho(r)/dr \leq 0$) by

$$|F(x)|^2 = -\frac{1}{\rho_0(x)}\frac{d\rho(r)}{dr}\bigg|_{r=x} \tag{12}$$

being normalized as

$$\int_0^\infty dx|F(x)|^2 = 1. \tag{13}$$

In the case of the Brueckner method for nuclear matter energy [21,28,29] the symmetry energy $S^{NM}(x)$ of NM with density $\rho_0(x)$ is (see, e.g., Refs. [49,54]):

$$S^{NM}(x) = 41.7\rho_0^{2/3}(x) + b_4\rho_0(x) + b_5\rho_0^{4/3}(x) + b_6\rho_0^{5/3}(x). \tag{14}$$

Then, correspondingly, the asymmetric incompressibility has the form [49,50]:

$$\Delta K^{NM}(x) = -83.4\rho_0^{2/3}(x) + 4b_5\rho_0^{4/3}(x) + 10b_6\rho_0^{5/3}(x). \tag{15}$$

The expression for the energy density of the method of Brueckner [28,29] (see also [49,50,65]), which is used to obtain Equations (14) and (15) from Equations (3) and (5), correspondingly, contains the following values of the parameters:

$$\begin{aligned} b_1 &= -741.28, \quad b_2 = 1179.89, \quad b_3 = -467.54, \\ b_4 &= 148.26, \quad b_5 = 372.84, \quad b_6 = -769.57. \end{aligned} \tag{16}$$

According to the CDFM scheme, the symmetry energy and the curvature for finite nuclei can be expressed in the following forms:

$$s = \int_0^\infty dx|F(x)|^2 S^{NM}(x), \tag{17}$$

$$\Delta K = \int_0^\infty dx|F(x)|^2 \Delta K^{NM}(x). \tag{18}$$

In our calculations we apply self-consistent deformed Hartree–Fock method with density-dependent Skyrme interactions [66] with pairing correlations. We use the Skyrme SLy4 [67], Sk3 [68] and SGII [69] parametrizations (see also [49–52,54,70]). In addition, we probe the SkM parameter set [71], which led to an appropriate description of bulk nuclear properties. All necessary expressions for the single-particle functions and densities in the HF+BCS method can be found, e.g., in Ref. [49].

It is known that the value of the nuclear matter incompressibility ΔK^{NM} plays a key role in determining the location of the ISGMR centroid energy [59]. The different Skyrme parameter sets used in the present calculations are chosen since they are characterized by different values of the nuclear incompressibility, ΔK^{NM} = 230, 217, 215, and 355 MeV for SLy4, SkM, SGII, and Sk3, respectively, [72].

The mean square radii for protons and neutrons are defined as

$$< r^2_{\rm p,n} >= \frac{\int R^2 \rho_{\rm p,n}(\vec{R}) d\vec{R}}{\int \rho_{\rm p,n}(\vec{R}) d\vec{R}}. \tag{19}$$

The matter mean square radius $< r^2 >$ entering Equation (2) can be calculated by

$$< r^2 >= \frac{N}{A} < r^2_n > + \frac{Z}{A} < r^2_p > . \tag{20}$$

As shown in Section 2.1, there exist two ways to calculate the excitation energy of the giant monopole resonance. In both definitions the finite nuclei incompressibility ΔK (Equation (18)) is obtained within the CDFM. In the present work, describing the monopole vibrations in terms of harmonic oscillations of the nuclear size and assuming an $A^{1/3}$ law for it, we calculate E_{ISGMR} by using Equation (1). In it values of the parameter r_0 between 1.07 and 1.2 fm are adopted, which are determined from experiments on particle scattering off nuclei. If one applies definition (2), then the mean square mass radius (Equation (20)) has to be used.

3. Results and Discussion

Here we present the obtained results for the centroid energies of the ISGMR in finite nuclei extracted from nuclear matter many-body calculations using the Brueckner EDF. We show also their isotopic sensitivity for Ni, Sn, and Pb chains.

First, in Figure 1 we overlay, as examples, the density distributions of ^{56}Ni and ^{208}Pb and the corresponding CDFM weight function $|F(x)|^2$ as a function of x. As mentioned before, the densities are obtained in a self-consistent Hartree–Fock+BCS calculations with SLy4 interaction. The function $|F(x)|^2$ which is used in Equation (18) to obtain the incompressibility modulus, which is necessary to calculate the E_{ISGMR}, has the form of a bell with a maximum around $x = R_{1/2}$ at which the value of the density $\rho(x = R_{1/2})$ is around half of the value of the central density equal to ρ_c $[\rho(R_{1/2})/\rho_c = 0.5]$. It was shown in Refs. [54,57] that in this region around $\rho = \rho_c/2$ the values of $\Delta K^{NM}(\rho)$ take a significant part in the calculations. This fact is of particular importance and is related to the behavior of $S^{NM}(x)$ (Equation (14)) in the case of the Brueckner EDF showing its isospin instability (see Figure 1 of Ref. [57]), in contrast with other more realistic energy-density functionals. Therefore, to fully specify the role of both quantities $\Delta K^{NM}[\rho_0(x)]$ and $|F(x)|^2$ in the expression (18) for the finite nuclei incompressibility ΔK and to locate the relevant region of densities in finite nucleus calculations, we apply the same physical criterion related to the weight function $|F(x)|^2$, as in [57]. This is the width Γ of the weight function $|F(x)|^2$ at its half maximum (which is illustrated in Figure 1 on the example of ^{56}Ni and ^{208}Pb nuclei together with the corresponding distance in the density distribution $\rho(r)$), which is a good and acceptable choice. More specifically, we define the lower limit of integration as the lower value of the radius x, x_{min}, corresponding to the left point of the half-width Γ (for more details see the discussion in Refs. [54,57]). One can see also in Figure 1 the part of the density distribution $\rho(r)$ (at $r \geq x_{min}$) that is involved in the calculations.

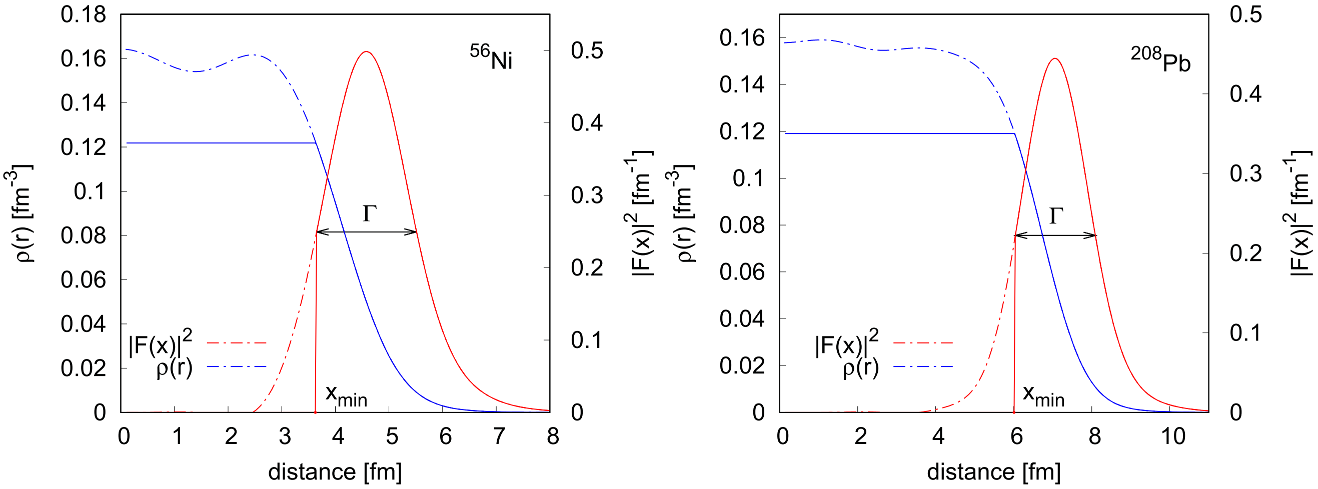

Figure 1. The densities $\rho(r)$ (in fm^{-3}) of ^{56}Ni and ^{208}Pb calculated in the Skyrme HF + BCS method with SLy4 force (normalized to $A = 56$ and $A = 208$, respectively) and the weight function $|F(x)|^2$ (in fm^{-1}) normalized to unity (Equation (13)).

The centroid positions of the monopole mode obtained in this work are compared with available experimental data in Tables 1–3. The calculated values of E_{ISGMR} with SLy4 and SkM forces for Ni and Pb isotopes are given in Tables 1 and 3, respectively. The values of the centroid energies for Sn isotopes obtained from calculations with three Skyrme interactions (SLy4, SGII, Sk3) are listed in Table 2. It can be seen from Table 1 that a very good agreement with the experimental data for ^{56,58,60}Ni is obtained, while the results with both Skyrme interactions underestimate the experimental energy of the soft monopole vibrations of ^{68}Ni. The excitation energy of this ISGMR in ^{68}Ni is located unexpectedly at higher energy (21.1 MeV) for the Ni isotopic chain, having at the same time large error bars. The reason is due to the large fragmentation of the isoscalar monopole strength in the unstable neutron-rich ^{68}Ni nucleus, much more than in stable nuclei [10,11]. The obtained values of E_{ISGMR} for Sn isotopes (A = 112–124) exhibit small difference regarding the Skyrme parametrization (see Table 2). The theoretical results for the centroid energies for the same Sn isotopes obtained in Ref. [59] by using the SkP (between 14.87 and 15.60 MeV), SkM* (between 15.57 and 16.23 MeV), and SLy5 (between 15.95 and 16.61 MeV) parameter sets are in good agreement with our results. Almost no dependence on the Skyrme forces used in the calculations of the centroid energies is found for Ni and Pb isotopes being slightly larger in the case of SkM interaction than when using the SLy4 one.

Table 1. The values of the centroid energies E_{ISGMR} (in MeV) of Ni isotopes obtained from HF+CDFM calculations in this work using SLy4 and SkM Skyrme forces compared with the experimental data found in the literature.

Nucleus	SLy4	SkM	Exp.
^{56}Ni	19.41	19.57	19.1 ± 0.5 [9]
			19.3 ± 0.5 [8]
^{58}Ni	18.95	19.18	18.43 ± 0.15 [58]
^{60}Ni	18.62	18.79	18.10(29) [58]
^{68}Ni	17.46	17.70	21.1 ± 1.9 [10,11]

Table 2. The values of the centroid energies E_{ISGMR} (in MeV) of Sn isotopes (A = 112–124) obtained from HF+CDFM calculations in this work using SLy4, SGII, and Sk3 Skyrme forces. The experimental data are taken from Table III of Ref. [59].

Nucleus	SLy4	SGII	Sk3	Exp.
^{112}Sn	15.04	15.30	14.89	16.2 ± 0.1
^{114}Sn	15.03	15.20	14.70	16.1 ± 0.1
^{116}Sn	14.94	15.08	14.56	15.8 ± 0.1
^{118}Sn	14.82	15.13	14.48	15.8 ± 0.1
^{120}Sn	14.69	15.08	14.58	15.7 ± 0.1
^{122}Sn	14.68	15.00	14.61	15.4 ± 0.1
^{124}Sn	14.68	14.96	14.51	15.3 ± 0.1

Table 3. The values of the centroid energies E_{ISGMR} (in MeV) of Pb isotopes obtained from HF+CDFM calculations in this work using SLy4 and SkM Skyrme forces compared with the experimental data found in the literature.

Nucleus	SLy4	SkM	Exp.	Theory
^{204}Pb	12.16	12.29	13.98 [60]	
^{206}Pb	12.12	12.23	13.94 [60]	
^{208}Pb	12.10	12.15	13.96 ± 0.2 [61]	14.453 [23]

The collective (bulk) character of the giant resonances and nuclear incompressibility presumes a quite smooth variation of the properties of the ISGMR with mass, thus not expecting very strong variations related to the internal nuclear structure. The isotopic evolution of the centroid energies E_{ISGMR} for the Ni, Sn, and Pb isotopes is presented in Figure 2 in the case when $r_0 = 1.2$ fm is used. In general, as expected, a smooth decrease in the excitation energies of the ISGMR with the increase in the mass number A is observed for the three isotopic chains and for all Skyrme forces used in the calculations. Furthermore, going from Ni to Pb isotopic chain the "gap" between our results and the corresponding experimental data becomes larger in a way that the obtained values of E_{ISGMR} underestimate the experimentally extracted values. Nevertheless, this difference does not exceed 1–2 MeV in the case of Sn and Pb isotopes and practically is minimal for Ni isotopes.

As a test of the role of the half-density radius parameter r_0 on the centroid energy (Equation (1)), we present in Figure 3 the results of E_{ISGMR} for the same Ni, Sn, and Pb isotopic chains in the case of SLy4 force obtained with two more values of r_0. In addition to the results with $r_0 = 1.2$ fm (e.g., in Refs. [73,74]) given in Figure 2, the values of E_{ISGMR} calculated with $r_0 = 1.07$ fm (for instance, in Ref. [75]) and $r_0 = 1.123$ fm [76] are shown in Figure 3. It is seen from the figure that with the increase of r_0 the agreement with the experimental data becomes better for lighter isotopes. Particularly, the value of $r_0 = 1.123$ fm leads to fair agreement of the ISGMR energies for Sn isotopes, while for Ni isotopes the experimental data are reproduced better with $r_0 = 1.2$ fm and for Pb isotopes with $r_0 = 1.07$ fm. Here we would like to note that the specific choice of the r_0 parameter values adopted to calculate the values of the centroid energies by using expression (1) is often used in the literature. The values of the measured nuclear radii are deduced from processes with strongly interacting particles or electron (muon) scattering. It is well known that the A-dependence of r_0 exhibits a smooth decrease with A being 1.07 fm for nuclei with $A > 16$ and increasing to 1.2 fm for heavy nuclei. This results on the calculated values of E_{ISGMR} and the corresponding ranges of change in respect to r_0 are illustrated in Figure 3 by hatched areas. Thus, we find a sensitivity of the results for centroid energies of ISGMR to the radial parameter r_0 and this fact has to be taken into account when considering resonances in light, medium, and heavy nuclei.

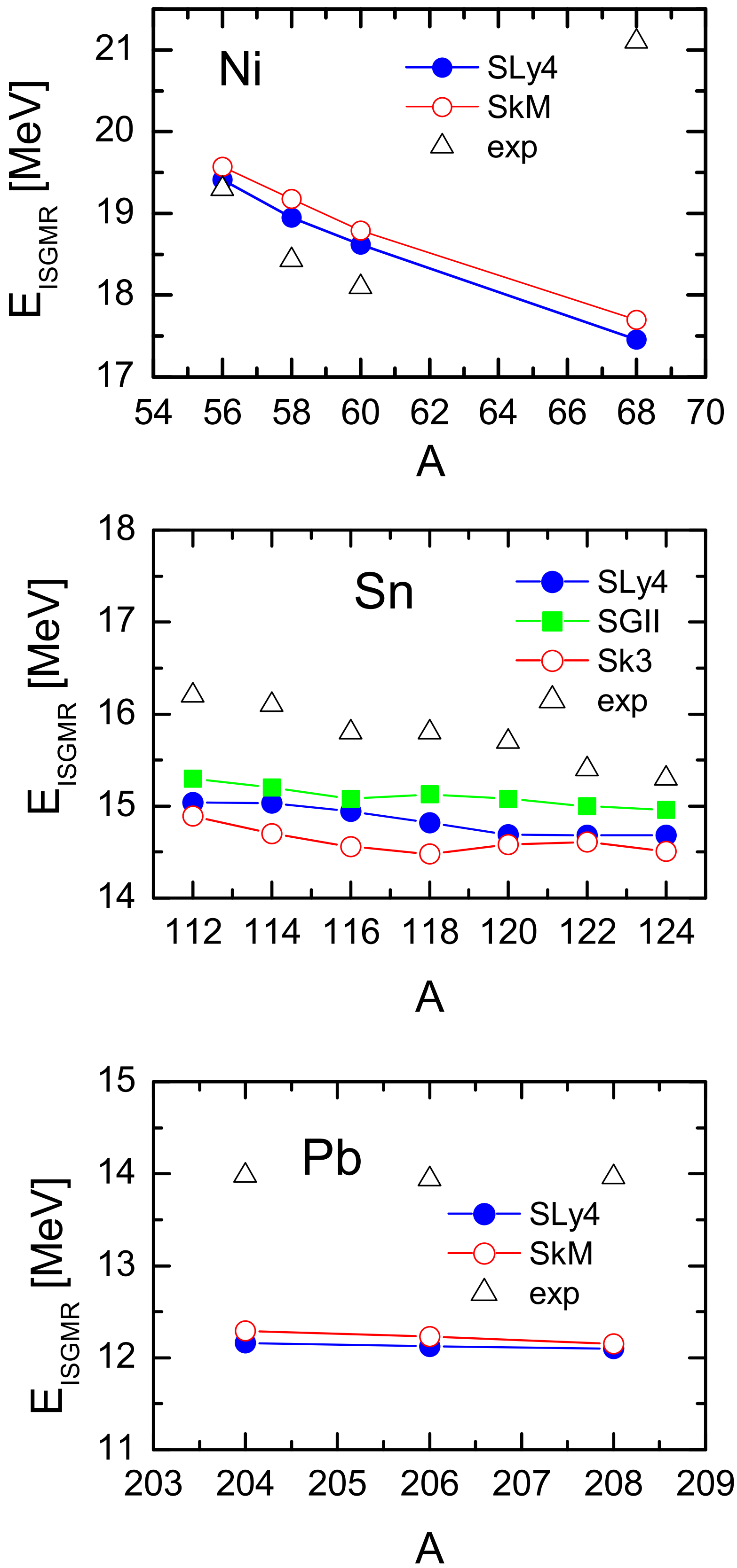

Figure 2. The centroid energies E_{ISGMR} as a function of the mass number A for Ni, Sn, and Pb isotopes in the cases of SLy4, SGII, Sk3, and SkM forces and $r_0 = 1.2$ fm (Equation (1)) compared with the experimental data.

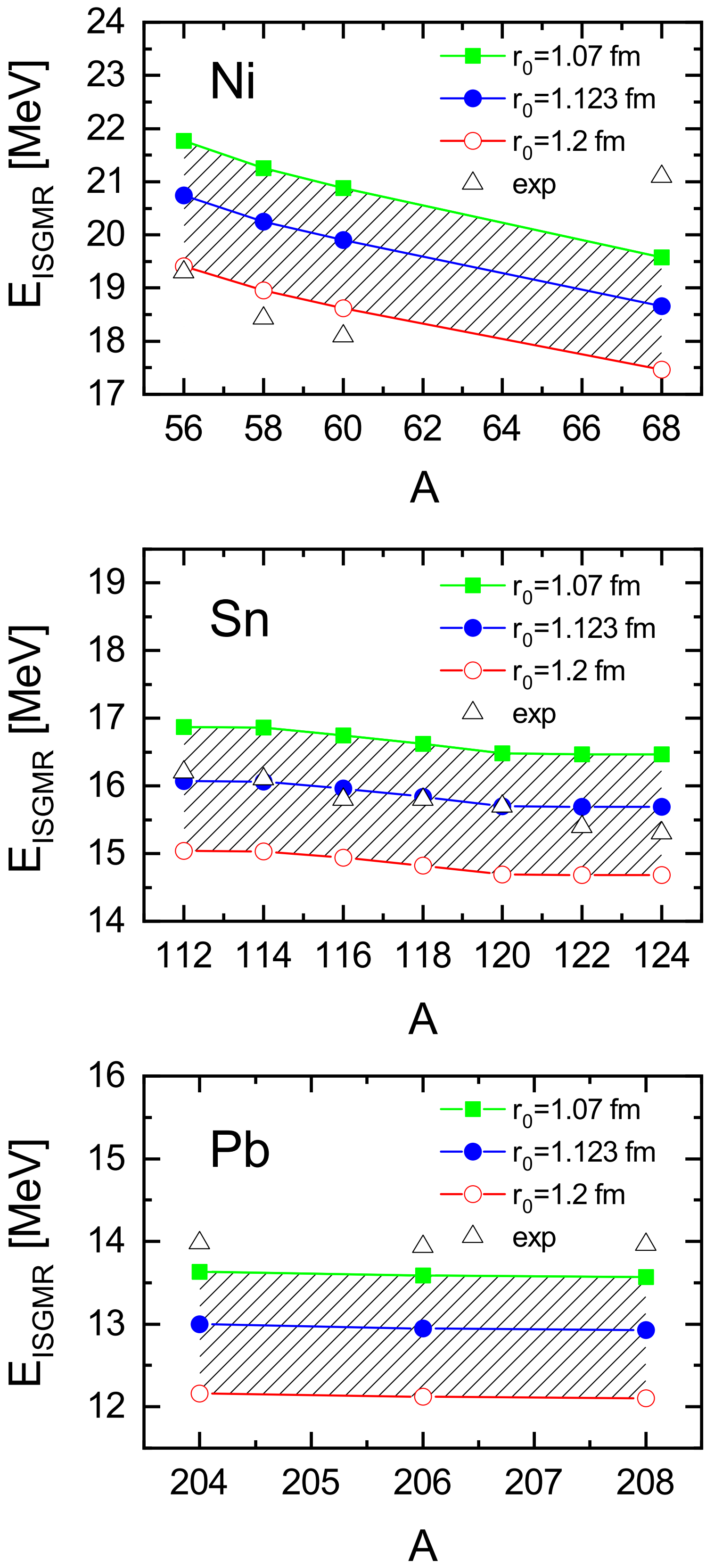

Figure 3. The centroid energies E_{ISGMR} as a function of the mass number A for Ni, Sn, and Pb isotopes in the case of SLy4 force obtained with three different values of the parameter $r_0 = 1.07, 1.123, 1.2$ fm (Equation (1)) compared with the experimental data.

4. Conclusions and Perspectives

We have performed a systematic study of the isoscalar giant monopole resonance in Ni, Sn, and Pb isotopes within the microscopic self-consistent Skyrme HF+BCS method and coherent density fluctuation model. In the present calculations four different Skyrme parameter sets are used: SLy4, SGII, Sk3, and SkM. They are chosen since they were employed in our previous works and, more importantly, are characterized by different values of the nuclear matter incompressibility. The calculations are based on the Brueckner energy-density functional for nuclear matter.

A very good agreement is achieved between the calculated centroid energies of the ISGMR and corresponding experimental values for Ni isotopes when $r_0 = 1.2$ fm. Especially this concerns the exotic double-magic ^{56}Ni nucleus, for which the obtained (with SLy4 Skyrme force) value is 19.41 MeV, in consistency with the centroid position of the ISGMR found at 19.1 ± 0.5 MeV. For ^{68}Ni our predictions for E_{ISGMR} with both Skyrme interactions are rather below the experimental result, obviously requiring a larger value of ΔK. The comparative analysis of the centroid energies in the case of Sn and Pb isotopes shows less agreement with $r_0 = 1.2$ fm, but still in an acceptable limits. This could be partly due to the chosen physical criterion that is applied to calculate the finite nucleus incompressibility (Equation (18)). The latter point will be a subject of future study. The agreement with the experimental values of E_{ISGMR} can be improved also by varying the parameter r_0 (Equation (1)) in strong connection with the mass dependence of this parameter and its effect for the considered isotopes.

In general, the results obtained in the present work demonstrate the relevance of our theoretical approach to probe the excitation energy of the ISGMR in various nuclei. Our future goal is to extend this theoretical study by employing more realistic energy-density functionals for nuclear matter, from one side. For example, the role of microscopic three-body forces in the proposed approach to study the giant monopole resonances can be clearly revealed by applying the latest version of the Barcelona–Catania–Paris–Madrid nuclear EDF ([77] and references therein) and particularly to treat successfully medium-heavy nuclei. In addition, a good choice could be the microscopic EOS derived by Sammarruca et al. [78] based on high-precision chiral nucleon-nucleon potentials at next-to-next-to-next-to-leading order (N^{3}LO) of chiral perturbation theory [79,80]. Thus, by employing of microscopic input in the energy-density functionals for nuclear matter, a stronger connection with fundamental nuclear forces can be achieved. From another side, the important issue will be to expand the nuclear spectrum to lighter and medium mass nuclei considering also deformed nuclei, in which the breaking of spherical symmetry would play a role. In addition, to extract the isospin dependence of the incompressibility coefficient, a key ingredient in astrophysical studies, further theoretical investigations are needed to carry out calculations of the ISGMR for neutron-rich nuclei and to compare the results with the available experimental data.

Author Contributions: Conceptualization, M.K.G., M.V.I. and A.N.A.; Formal analysis, M.K.G., M.V.I. and A.N.A.; Visualization, M.K.G. and M.V.I.; Writing-original draft, M.K.G.; Writing-review and editing, M.K.G., M.V.I., Y.I.K. and A.N.A. All authors have read and agreed to the published version of the manuscript.

Funding: This research was funded by the Bulgarian National Science Fund under Contract No. KP-06-N38/1.

Institutional Review Board Statement: Not applicable.

Informed Consent Statement: Not applicable.

Data Availability Statement: Not applicable.

Conflicts of Interest: The authors declare no conflict of interest.

References

1. Bohr, A.; Mottelson, B. *Nuclear Structure*; Benjamin: New York, NY, USA, 1975; Volume 2.
2. Harakeh, M.N.; van der Woude, A. *Giant Resonances*; Oxford University Press: Oxford, UK, 2001.
3. Brandenburg, S.; Leo, R.D.; Drentje, A.G.; Harakeh, M.N.; Janszen, H.; van der Woude, A. Fission decay of the isoscalar giant monopole resonance in ^{238}U. *Phys. Rev. Lett.* **1982**, *49*, 1687. [CrossRef]
4. Zwarts, F.; Drentje, A.; Harakeh, M.; van der Woude, A. The isoscalar quadrupole strength distribution above 10 MeV in ^{40}Ca. *Phys. Lett. B* **1983**, *125*, 123. [CrossRef]
5. Brandenburg, S.; Leo, R.D.; Drentje, A.; Harakeh, M.; Sakai, H.; van der Woude, A. Experimental determination of monopole strength in ^{40}Ca between 10 and 20 MeV excitation energy. *Phys. Lett. B* **1983**, *130*, 9. [CrossRef]
6. Shlomo, S.; Youngblood, D.H. Nuclear matter compressibility from isoscalar giant monopole resonance. *Phys. Rev. C* **1993**, *47*, 529. [CrossRef] [PubMed]
7. Youngblood, D.H.; Clark, H.L.; Lui, Y.-W. Incompressibility of nuclear matter from the giant monopole resonance. *Phys. Rev. Lett.* **1999**, *82*, 691. [CrossRef]
8. Monrozeau, C.; Khan, E.; Blumenfeld, Y.; Demonchy, C.E.; Mittig, W.; Roussel-Chomaz, P.; Beaumel, D.; Caamaño, M.; Cortina-Gil, D.; Ebran, J.P.; et al. First measurement of the giant monopole and quadrupole resonances in a short-lived nucleus: ^{56}Ni. *Phys. Rev. Lett* **2008**, *100*, 042501. [CrossRef] [PubMed]
9. Bagchi, S.; Gibelin, J.; Harakeh, M.N.; Kalantar-Nayestanaki, N.; Achouri, N.L.; Akimune, H.; Bastin, B.; Boretzky, K.; Bouzomita, H.; Caamano, M.; et al. Observation of isoscalar multipole strengths in exotic doubly-magic ^{56}Ni in inelastic α scattering in inverse kinematics. *Phys. Lett. B* **2015**, *751*, 371. [CrossRef]
10. Vandebrouck, M.; Gibelin, J.; Khan, E.; Achouri, N.L.; Baba, H.; Beaumel, D.; Blumenfeld, Y.; Caamaño, M.; Càceres, L.; Colò, G.; et al. Measurement of the isoscalar monopole response in the neutron-rich nucleus ^{68}Ni. *Phys. Rev. Lett.* **2014**, *113*, 032504. [CrossRef] [PubMed]
11. Vandebrouck, M.; Gibelin, J.; Khan, E.; Achouri, N.L.; Baba, H.; Beaumel, D.; Blumenfeld, Y.; Caamano, M.; Caceres, L.; Colo, G.; et al. Isoscalar response of ^{68}Ni to α-particle and deuteron probes. *Phys. Rev. C* **2015**, *92*, 024316. [CrossRef]
12. Blaizot, J.P. Nuclear comressibilities. *Phys. Rep.* **1980**, *64*, 171. [CrossRef]
13. Garg, U.; Colò, G. The compression-mode giant resonances and nuclear incompressibility. *Prog. Part. Nucl. Phys.* **2018**, *101*, 55. [CrossRef]
14. Li, T.; Garg, U.; Liu, Y.; Marks, R.; Nayak, B.K.; Rao, P.M.; Fujiwara, M.; Hashimoto, H.; Nakanishi, K.; Okumura, S.; et al. Isoscalar giant resonances in the Sn nuclei and implications for the asymmetry term in the nuclear-matter incompressibility. *Phys. Rev. C* **2010**, *81*, 034309. [CrossRef]
15. Patel, D.; Garg, U.; Fujiwara, M.; Akimune, H.; Berg, G.P.A.; Harakeh, M.N.; Itoh, M.; Kawabata, T.; Kawase, K.; Nayak, B.K.; et al. Giant monopole resonance in even-A Cd isotopes, the asymmetry term in nuclear incompressibility, and the "softness" of Sn and Cd nuclei. *Phys. Lett. B* **2012**, *718*, 447. [CrossRef]
16. Blaizot, J.P.; Gogny, D.; Grammaticos, B. Nuclear compressibility and monopole resonances. *Nucl. Phys. A* **1976**, *265*, 315. [CrossRef]
17. Button, J.; Lui, Y.-W.; Youngblood, D.H.; Chen, X.; Bonasera, G.; Shlomo, S. Isoscalar $E0$, $E1$, and $E2$ strength in ^{44}Ca. *Phys. Rev. C* **2017**, *96*, 054330. [CrossRef]
18. Howard, K.B.; Garg, U.; Gupta, Y.K.; Harakeh, M.N. Where we stand on structure dependence of ISGMR in the Zr-Mo region: Implications on K_∞. *Eur. Phys. J. A* **2019**, *55*, 228. [CrossRef]
19. Howard, K.B.; Garg, U.; Itoh, M.; Akimune, H.; Bagchi, S.; Doi, T.; Fujikawa, Y.; Fujiwara, M.; Furuno, T.; Harakeh, M.N.; et al. Compression-mode resonances in the calcium isotopes and implications for the asymmetry term in nuclear incompressibility. *Phys. Lett. B* **2020**, *801*, 135185. [CrossRef]
20. Howard, K.B.; Garg, U.; Itoh, M.; Akimune, H.; Fujiwara, M.; Furuno, T.; Gupta, Y.K.; Harakeh, M.N.; Inaba, K.; Ishibashi, Y.; et al. Compressional-mode resonances in the molybdenum isotopes: Emergence of softness in open-shell nuclei near A = 90. *Phys. Lett. B* **2020**, *807*, 135608. [CrossRef]
21. Brueckner, K.A.; Giannoni, M.J.; Lombard, R.J. Statistical estimate of the breathing mode energy. *Phys. Lett.* **1970**, *31B*, 97. [CrossRef]
22. Shlomo, S. Compression modes and the nuclear matter incompressibility coefficient. *Pramana-J. Phys.* **2001**, *57*, 557. [CrossRef]
23. Chen, L.-W.; Gu, J.-Z. Correlations between the nuclear breathing mode energy and properties of asymmetric nuclear matter. *J. Phys. G* **2012**, *39*, 035104. [CrossRef]
24. Anders, M.R.; Shlomo, S. Giant resonances in ^{40}Ca and ^{48}Ca. *J. Phys. Conf. Ser.* **2013**, *420*, 012051. [CrossRef]
25. Su, J.; Zhu, L.; Guo, C. Isoscalar giant monopole resonance within the Bohr-Mottelson model. *Phys. Rev. C* **2018**, *98*, 024315. [CrossRef]
26. Colò, G.; Gambacurta, D.; Kleinig, W.; Kvasil, J.; Nesterenko, V.O.; Pastore, A. Isoscalar monopole and quadrupole modes in Mo isotopes: Microscopic analysis. *Phys. Lett. B* **2020**, *811*, 135940. [CrossRef]
27. Bonasera, G.; Shlomo, S.; Youngblood, D.H.; Lui, Y.-W.; Button, J.; Chen, X. Isoscalar and isovector giant resonances in ^{44}Ca, ^{54}Fe, ^{64,68}Zn and ^{56,58,60,68}Ni. *Nucl. Phys. A* **2021**, *1010*, 122159. [CrossRef]
28. Brueckner, K.A.; Buchler, J.R.; Jorna, S.; Lombard, A.R.J. Statistical theory of nuclei. *Phys. Rev.* **1968**, *171*, 1188. [CrossRef]

29. Brueckner, K.A.; Buchler, J.R.; Clark, R.C.; Lombard, A.R.J. Statistical theory of nuclei. II. Medium and heavy nuclei. *Phys. Rev.* **1969**, *181*, 1543. [CrossRef]
30. Antonov, A.N.; Nikolaev, V.A.; Petkov, I.Z. A model of coherent fluctuations of nuclear density. *Bulg. J. Phys.* **1979**, *6*, 151.
31. Antonov, A.N.; Nikolaev, V.A.; Petkov, I.Z. Nucleon momentum and density distributions in nuclei. *Z. Phys. A* **1980**, *297*, 257. [CrossRef]
32. Antonov, A.N.; Nikolaev, V.A.; Petkov, I.Z. Spectral functions and hole nuclear states. *Z. Phys. A* **1982**, *304*, 239. [CrossRef]
33. Antonov, A.N.; Nikolaev, V.A.; Petkov, I.Z. Extreme breathing excitations of atomic nuclei. *Nuovo Cimento A* **1985**, *86*, 23. [CrossRef]
34. Antonov, A.N.; Nikolov, E.N.; Christov, C.V.; Hodgson, P.E. Natural orbitals and occupation numbers in the coherent density fluctuation model. *Nuovo Cimento A* **1989**, *102*, 1701. [CrossRef]
35. Antonov, A.N.; Kadrev, D.N.; Hodgson, P.E. The effect of nucleon oorrelations on natural orbitals. *Phys. Rev. C* **1994**, *50*, 164. [CrossRef] [PubMed]
36. Antonov, A.N.; Hodgson, P.E.; Petkov, I.Z. *Nucleon Momentum and Density Distributions in Nuclei*; Clarendon Press: Oxford, UK, 1988.
37. Antonov, A.N.; Hodgson, P.E.; Petkov, I.Z. *Nucleon Correlations in Nuclei*; Springer: Berlin/Heidelberg Germany; New York, NY, USA, 1993.
38. Griffin, J.J.; Wheeler, J.A. Collective motions in nuclei by the method of generator coordinates. *Phys. Rev.* **1957**, *108*, 311. [CrossRef]
39. Antonov, A.N.; Bonev, I.S.; Christov, C.V.; Petkov, I.Z. Generator coordinate method calculations of nucleon momentum and density distributions in ^{4}He, ^{16}O and ^{40}Ca. *Nuovo Cimento A* **1988**, *100*, 779. [CrossRef]
40. Antonov, A.N.; Nikolaev, V.A.; Petkov, I.Z. Breathing monopole nuclear vibrations within the coherent density fluctuation model. *Bulg. J. Phys*. **1991**, *18*, 107.
41. Antonov, A.N.; Gaidarov, M.K.; Kadrev, D.N.; Ivanov, M.V.; Moya de Guerra, E.; Udias, J.M. Superscaling in nuclei: A search for scaling function beyond the relativistic Fermi gas model. *Phys. Rev. C* **2004**, *69*, 044321. [CrossRef]
42. Antonov, A.N.; Gaidarov, M.K.; Ivanov, M.V.; Kadrev, D.N.; Moya de Guerra, E.; Sarriguren, P.; Udias, J.M. Superscaling, scaling functions and nucleon momentum distributions in nuclei. *Phys. Rev.* C **2005**, *71*, 014317. [CrossRef]
43. Antonov, A.N.; Ivanov, M.V.; Gaidarov, M.K.; Moya de Guerra, E.; Sarriguren, P.; Udias, J.M. Scaling functions and superscaling in medium and heavy nuclei. *Phys. Rev. C* **2006**, *73*, 047302. [CrossRef]
44. Antonov, A.N.; Ivanov, M.V.; Gaidarov, M.K.; Moya de Guerra, E.; Caballero, J.A.; Barbaro, M.B.; Udias, J.M.; Sarriguren, P. Superscaling analysis of inclusive electron scattering and its extension to charge-changing neutrino cross sections in nuclei. *Phys. Rev. C* **2006**, *74*, 054603. [CrossRef]
45. Ivanov, M.V.; Barbaro, M.B.; Caballero, J.A.; Antonov, A.N.; Moya de Guerra, E.; Gaidarov, M.K. Superscaling and charge-changing neutrino scattering from nucle in the Δ region beyond the relativistic Fermi gas model. *Phys. Rev. C* **2008**, *77*, 034612. [CrossRef]
46. Antonov, A.N.; Ivanov, M.V.; Barbaro, M.B.; Caballero, J.A.; Moya de Guerra, E.; Gaidarov, M.K. Superscaling and neutral current quasielastic neutrino-nucleus scattering beyond the relativistic Fermi gas model. *Phys. Rev. C* **2007**, *75*, 064617. [CrossRef]
47. Antonov, A.N.; Ivanov, M.V.; Barbaro, M.B.; Caballero, J.A.; Moya de Guerra, E. Longitudinal and transverse scaling functions within the coherent density fluctuation model. *Phys. Rev. C* **2009**, *79*, 044602. [CrossRef]
48. Caballero, J.A.; Barbaro, M.B.; Antonov, A.N.; Ivanov, M.V.; Donnelly, T.W. Scaling function and nucleon momentum distribution. *Phys. Rev. C* **2010**, *81*, 055502. [CrossRef]
49. Gaidarov, M.K.; Antonov, A.N.; Sarriguren, P.; Moya de Guerra, E. Surface properties of neutron-rich exotic nuclei: A source for studying the nuclear symmetry energy. *Phys. Rev. C* **2011**, *84*, 034316. [CrossRef]
50. Gaidarov, M.K.; Antonov, A.N.; Sarriguren, P.; Moya de Guerra, E. Symmetry energy of deformed neutron-rich nuclei. *Phys. Rev. C* **2012**, *85*, 064319. [CrossRef]
51. Gaidarov, M.K.; Sarriguren, P.; Antonov, A.N.; Moya de Guerra, E. Ground-state properties and symmetry energy of neutron-rich and neutron-deficient Mg isotopes. *Phys. Rev. C* **2014**, *89*, 064301. [CrossRef]
52. Antonov, A.N.; Gaidarov, M.K.; Sarriguren, P.; Moya de Guerra, E. Volume and surface contributions to the nuclear symmetry energy within the coherent density fluctuation model. *Phys. Rev. C* **2016**, *94*, 014319. [CrossRef]
53. Antonov, A.N.; Kadrev, D.N.; Gaidarov, M.K.; Sarriguren, P.; Moya de Guerra, E. Temperature dependence of the volume and surface contributions to the nuclear symmetry energy within the coherent density fluctuation model. *Phys. Rev. C* **2018**, *98*, 054315. [CrossRef]
54. Danchev, I.C.; Antonov, A.N.; Kadrev, D.N.; Gaidarov, M.K.; Sarriguren, P.; Moya de Guerra, E. Symmetry energy properties of neutron-rich nuclei from the coherent density fluctuation model applied to nuclear matter calculations with Bonn potentials. *Phys. Rev. C* **2020**, *101*, 064315. [CrossRef]
55. Gaidarov, M.K.; Moumene, I.; Antonov, A.N.; Kadrev, D.N.; Sarriguren, P.; Moya de Guerra, E. Proton and neutron skins and symmetry energy of mirror nuclei. *Nucl. Phys. A* **2020**, *1004*, 122061. [CrossRef]
56. Gaidarov, M.K.; Antonov, A.N.; Kadrev, D.N.; Sarriguren, P.; Moya de Guerra, E.Chapter in *Nuclear Structure Physics*; Shukla, A., Patra, S.K., Eds.; CRC Press: Boca Raton, FL, USA; Taylor & Francis Group: Abingdon, UK, 2020; pp. 93–120.
57. Gaidarov, M.K.; de Guerra, M.; Antonov, A.N.; Danchev, I.C.; Sarriguren, P.; Kadrev, D.N. Nuclear symmetry energy components and their ratio: A new approach within the coherent density fluctuation model. *Phys. Rev. C* **2021**, *104*, 044312. [CrossRef]

58. Lui, Y.-W.; Youngblood, D.H.; Clark, H.L.; Tokimoto, Y.; John, B. Isoscalar giant resonances for nuclei with mass between 56 and 60. *Phys. Rev. C* **2006**, *73*, 014314. [CrossRef]
59. Cao, L.-G.; Sagawa, H.; Colò, G. Microscopic study of the isoscalar giant monopole resonance in Cd, Sn, and Pb isotopes. *Phys. Rev. C* **2012**, *86*, 054313. [CrossRef]
60. Fujiwara, M.; Li, T.; Patel, D.; Garg, U.; Berg, G.P.A.; Liu, Y.; Marks, R.; Matta, J.; Nayak, B.K.; Madhusudhana-Rao, P.V.; et al. Measurements of ISGMR in Sn, Cd and Pb isotopes and the asymmetry of nuclear matter incompressibility. *AIP Conf. Proc.* **2011**, *1377*, 164.
61. Youngblood, D.H.; Lui, Y.-W.; Clark, H.L.; John, B.; Tokimoto, Y.; Chen, X. Isoscalar $E0$-$E3$ strength in ^{116}Sn, ^{144}Sm, ^{154}Sm, and ^{208}Pb. *Phys. Rev. C* **2004**, *69*, 034315. [CrossRef]
62. Stringari, S. Sum rules for compression modes. *Phys. Lett. B* **1982**, *108*, 232. [CrossRef]
63. Dieperink, A.E.L.; Dewulf, Y.; Van Neck, D.; Waroquier, M.; Rodin, V. Nuclear symmetry energy and the neutron skin in neutron-rich nuclei. *Phys. Rev. C* **2003**, *68*, 064307. [CrossRef]
64. Chen, l.W. Nuclear matter symmetry energy and the symmetry energy coefficient in the mass formula. *Phys. Rev. C* **2011**, *83*, 044308. [CrossRef]
65. Bethe, H.A. Theory of Nuclear Matter. *Annu. Rev. Nucl. Sci.* **1971**, *21*, 93. [CrossRef]
66. Vautherin, D. Hartree-Fock calculations with Skyrme's interaction. II. Axially deformed nuclei. *Phys. Rev. C* **1973**, *7*, 296. [CrossRef]
67. Chabanat, E.; Bonche, P.; Haensel, P.; Meyer, J.; Schaeffer, R. A Skyrme parametrization from subnuclear to neutron star densities Part II. Nuclei far from stabilities. *Nucl. Phys. A* **1998**, *635*, 231. [CrossRef]
68. Beiner, M.; Flocard, H.; Giai, N.V.; Quentin, P. Nuclear ground-state properties and self-consistent calculations with the Skyrme interaction (I). Spherical description. *Nucl. Phys. A* **1975**, *238*, 29. [CrossRef]
69. Giai, N.V.; Sagawa, H. Spin-isospin and pairing properties of modified Skyrme interactions. *Phys. Lett. B* **1981**, *106*, 379. [CrossRef]
70. Sarriguren, P.; Gaidarov, M.K.; de Guerra, E.M.; Antonov, A.N. Nuclear skin emergence in Skyrme deformed Hartree-Fock calculations. *Phys. Rev. C* **2007**, *76*, 044322. [CrossRef]
71. Krivine, H.; Treiner, J.; Bohigas, O. Derivation of a fluid-dynamical lagrangian and electric giant resonances. *Nucl. Phys. A* **1980**, *336*, 155. [CrossRef]
72. Danielewicz, P.; Lee, J. Symmetry energy I: Semi-infinite matter. *Nucl. Phys. A* **2009**, *818*, 36. [CrossRef]
73. Brown, B.A.; Bronk, C.R.; Hodgson, P.E. Systematics of nuclear rms charge radii. *J. Phys. G* **1984**, *10*, 1683. [CrossRef]
74. Li, R.-H.; Hu, Y.-M.; Li, M.-C. An analysis of nuclear charge radii based on the empirical formula. *Chin. Phys. C* **2009**, *33*, 123.
75. Walecka, J.D. *Theoretical Nuclear and Subnuclear Physics*; Oxford University Press: Oxford, NY, USA, 1995.
76. Eisenberg, J.M.; Greiner, W. Nuclear Theory. In *Excitation Mechanusms of the Nucleus*; North-Holland Publishing Company: Amsterdam, The Netherlands; London, UK, 1970; Volume 2.
77. Sharma, B.K.; Centelles, M.; Vi nas, X.; Baldo, M.; Burgio, G.F. Unified equation of state for neutron stars on a microscopic basis. *Astron. Astrophys.* **2015**, *584*, A103. [CrossRef]
78. Sammarruca, F.; Coraggio, L.; Holt, J.W.; Itaco, N.; Machleidt, R.; Marcucci, L.E. Toward order-by-order calculations of the nuclear and neutron matter equations of state in chiral effective field theory. *Phys. Rev. C* **2015**, *91*, 054311. [CrossRef]
79. Machleidt, R.; Entem, D.R. Chiral effective field theory and nuclear forces. *Phys. Rep.* **2011**, *503*, 1. [CrossRef]
80. Entem, D.R.; Machleidt, R. Accurate charge-dependent nucleon-nucleon potential at fourth order of chiral perturbation theory. *Phys. Rev. C* **2003**, *68*, 041001(R). [CrossRef]